16

AlSb Compound Semiconductor as Absorber Layer in Thin Film Solar Cells

Rabin Dhakal, Yung Huh, David Galipeau and Xingzhong Yan
Department of Electrical Engineering and Computer Science, Department of Physics, South Dakota State University, Brookings SD 57007, USA

1. Introduction

Since industrial revolution by the end of nineteenth century, the consumption of fossil fuels to drive the economy has grown exponentially causing three primary global problems: depletion of fossil fuels, environmental pollution, and climate change (Andreev and Grilikhes, 1997). The population has quadrupled and our energy demand went up by 16 times in the 20th century exhausting the fossil fuel supply at an alarming rate (Bartlett, 1986; Wesiz, 2004). By the end of 2035, about 739 quadrillion Btu of energy (1 Btu = 0.2930711 W-hr) of energy would be required to sustain current lifestyle of 6.5 billion people worldwide (US energy information administration, 2010). The increasing oil and gas prices, gives us enough region to shift from burning fossil fuels to using clean, safe and environmentally friendly technologies to produce electricity from renewable energy sources such as solar, wind, geothermal, tidal waves etc (Kamat, 2007). Photovoltaic (PV) technologies, which convert solar energy directly into electricity, are playing an ever increasing role in electricity production worldwide. Solar radiation strikes the earth with 1.366 KWm^{-2} of solar irradiance, which amounts to about 120,000 TW of power (Kamat 2007). Total global energy needs could thus be met, if we cover 0.1% of the earth's surface with solar cell module with an area 1 m^2 producing 1KWh per day (Messenger and Ventre, 2004).

There are several primary competing PV technologies, which includes: (a) crystalline (c-Si), (b) thin film (a-Si, CdTe, CIGS), (c) organic and (d) concentrators in the market. Conventional crystalline silicon solar cells, also called first generation solar cells, with efficiency in the range of 15 - 21 %, holds about 85 % of share of the PV market (Carabe and Gandia, 2004). The cost of the electricity generation estimates to about $4/W which is much higher in comparison to $0.33/W for traditional fossil fuels (Noufi and Zweibel, 2006). The reason behind high cost of these solar cells is the use of high grade silicon and high vacuum technology for the production of solar cells. Second generation, thin film solar cells have the lowest per watt installation cost of about $1/W, but their struggle to increase the market share is hindered mainly due to low module efficiency in the range of 8-11% ((Noufi and Zweibel, 2006; Bagnall and Boreland, 2008). Increasing materials cost, with price of Indium more than $700/kg (Metal-pages, n.d.), and requirements for high vacuum processing have kept the cost/efficiency ratio too high to make these technologies the primary player in PV market (Alsema, 2000). Third generation technologies can broadly be divided in two categories: devices achieving high efficiency using novel approaches like concentrating and

tandem solar cells and moderately efficient organic based photovoltaic solar cells (Sean and Ghassan, 2005; Currie et al., 2008). The technology and science for third generation solar cells are still immature and subject of widespread research area in PV.

1.1 Thin film solar cells

Second Generation thin film solar cells (TFSC) are a promising approach for both the terrestrial and space PV application and offer a wide variety of choices in both device design and fabrication. With respect to single crystal silicon technology, the most important factor in determining the cost of production is the cost of 250-300 micron thick Si wafer (Chopra et al., 2004). Thin-film technologies allow for significant reduction in semiconductor thickness because of the capacity of certain materials for absorbing most of the incident sunlight within a few microns of thickness, in comparison to the several hundred microns needed in the crystalline silicon technology (Carabe and Gandia, 2004). In addition, thin-film technology has an enormous potential in cost reduction, based on the easiness to make robust, large-area monolithic modules with a fully automatic fabrication procedure. Rapid progress is thus made with inorganic thin-film PV technologies, both in the laboratory and in industry (Aberle, 2009).

Amorphous silicon based PV modules have been around for more than 20 years Chithik et al. first deposited amorphous silicon from a silane discharge in 1969 (Chittik et al., 1969) but its use in PV was not much progress, until Clarson found out a method to dope it n or p type in 1976 (Clarson, n.d.) Also, it was found that the band gap of amorphous silicon can be modified by changing the hydrogen incorporation during fabrication or by alloying a-Si with Ge or C (Zanzucchi et al., 1977; Tawada et al. 1981). This introduction of a-Si:C:H alloys as p-layer and building a hetero-structure device led to an increase of the open-circuit voltage into the 800 mV range and to an increased short-circuit current due to the "window" effect of the wideband gap p layer increasing efficiency up to 7.1% (Tawada et al. 1981, 1982). Combined with the use of textured substrates to enhance optical absorption by the "light trapping" effect, the first a-Si:H based solar cell with more than 10% conversion efficiency was presented in 1982 (Catalakro et al., 1982). However, there exists two primary reasons due to which a-Si:H has not been able to conquer a significant share of the global PV market. First is the low stable average efficiency of 6% or less of large-area single-junction PV modules due to "Staebler–Wronski effect", i.e. the light-induced degradation of the initial module efficiency to the stabilized module efficiency (Lechner and Schad, 2002; Staebler and Wronski, 1977). Second reason is the manufacturing related issues associated with the processing of large (>1 m^2) substrates, including spatial non-uniformities in the Si film and the transparent conductive oxide (TCO) layer (Poowalla and Bonnet, 2007).

Cadmium Telluride (CdTe) solar cell modules have commercial efficiency up to 10-11% and are very stable compound (Staebler and Wronski, 1977). CdTe has the efficient light absorption and is easy to deposit. In 2001, researches at National Renewable Energy Laboratory (NREL) reported an efficiency of 16.5% for these cells using chemical bath deposition and antireflective coating on the borosilicate glass substrate from $CdSnO_4$ (Wu et al., 2001). Although there has been promising laboratory result and some progress with commercialization of this PV technology in recent years (First Solar, n.d.), it is questionable whether the production and deployment of toxic Cd-based modules is sufficiently benign environmentally to justify their use. Furthermore, Te is a scarce element and hence, even if most of the annual global Te production is used for PV, CdTe PV module production seems limited to levels of a few GW per year (Aberle, 2009).

The CIGS thin film belongs to the multinary Cu-chalcopyrite system, where the bandgap can be modified by varying the Group III (on the Periodic Table) cations among In, Ga, and Al and the anions between Se and S (Rau and Schock, 1999). This imposes significant challenges for the realization of uniform film properties across large-area substrates using high-throughput equipment and thereby affects the yield and cost. Although CIGS technology is a star performer in laboratory, with confirmed efficiencies of up to 19.9% for small cells (Powalla and Bonnet, 2007) however the best commercial modules are presently 11–13% efficient (Green et al. 2008). Also there are issues regarding use of toxic element cadmium and scarcity of indium associated with this technology. Estimates indicate that all known reserves of indium would only be sufficient for the production of a few GW of CIGS PV modules (Aberle, 2009).

This has prompted researchers to look for new sources of well abundant, non toxic and inexpensive materials suitable for thin film technology. Binary and ternary compounds of group III-V and II-VI are of immediate concern when we look for alternatives. AlSb a group III-V binary compound is one of the most suitable alternatives for thin film solar cells fabrication because of its suitable optical and electrical properties (Armantrout et al., 1977). The crystalline AlSb film has theoretical conversion efficiency more than 27% as suggested in literature (Zheng et al., 2009).

1.2 Aluminum antimony thin films

Aluminum Antimony is a binary compound semiconductor material with indirect band gap of 1.62 eV thus ideal for solar spectrum absorption (Chandra et al., 1988). This also has become the material of interest due to relatively easy abundance and low cost of Al and Sb. AlSb single crystal has been fabricated from the Czochralski process but the AlSb thin film was prepared by Johnson et al. by co-evaporation of Al and Sb. They also studied the material properties to find out its donor and acceptor density and energy levels (Johnson, 1965). Francombe et al. observed the strong photovoltaic response in vacuum deposited AlSb for the first time in 1976 (Francombe et al., 1976). Number of research groups around the world prepared thin AlSb thin film and studied its electrical and optical properties by vacuum and non vacuum technique. These include, Leroux et al. deposited AlSb films on number of insulating substrate by MOCVD deposition technique in 1979 (Leroux et al., 1980). Dasilva et al. deposited AlSb film by molecular beam epitaxy and studied its oxidation by Auger and electron loss spectroscopy in 1991 (Dasilva et al., 1991). Similarly, AlSb film was grown by hot wall epitaxy and their electrical and optical properties was studied by Singh and Bedi in 1998 (Singh and Bedi, 1998). Chen et al. prepared the AlSb thin film by dc magnetron sputtering and studied its electrical and optical properties (Chen et al. 2008) in 2007. Gandhi et al. deposited AlSb thin film on by the alternating electrical pulses from the ionic solution of $AlCl_3$ and $SbCl_3$ in EMIC (1-methyl-3-ethylimidazolium chloride) and studied its electrical and optical characters (Gandhi et al. 2008). However, AlSb thin film had never been successfully employed as an absorber material in photovoltaic cells. We, electro-deposited AlSb thin film on the TiO_2 substrate by using the similar technique as Gandhi et al. and had observed some photovoltaic response in 2009 (Dhakal et al., 2009). Al and Sb ions are extremely corrosive and easily react with air and moisture. Thus it becomes very difficult to control the stoichiometry of compound while electroplating. Thus, vacuum deposition techniques become the first choice to prepare AlSb thin films for the solar cell applications. In this work, we fabricated AlSb thin film co-sputtering of Al and Sb target. The film with optimized band-gap was used to fabricate p-n and p-*i*-n device structures. The photovoltaic response of the devices was investigated.

2. Fabrication of AlSb thin films

AlSb film was prepared from dc magnetron sputtering of Al and Sb target (Kurt J. Lesker, Materials Group, PA) simultaneously in a sputtering chamber. Sputtering is a physical vapor deposition process whereby atoms are ejected from a solid target material due to bombardment of the target by plasma, a flow of positive ions and electrons in a quasi-neutral electrical state (Ohring, 2002). Sputtering process begins when the ion impact establishes a train of collision events in the target, leading to the ejection of a matrix atom (Ohring, 2002). The exact processes occurring at the target surface is depends on the energy of the incoming ions. Fig. 1 shows the schematic diagram of sputtering using DC and RF power. DC sputtering is achieved by applying large (~2000) DC voltages to the target (cathode) which establishes a plasma discharge as Ar^+ ions will be attracted to and impact the target. The impact cause sputtering off target atoms to substrates.

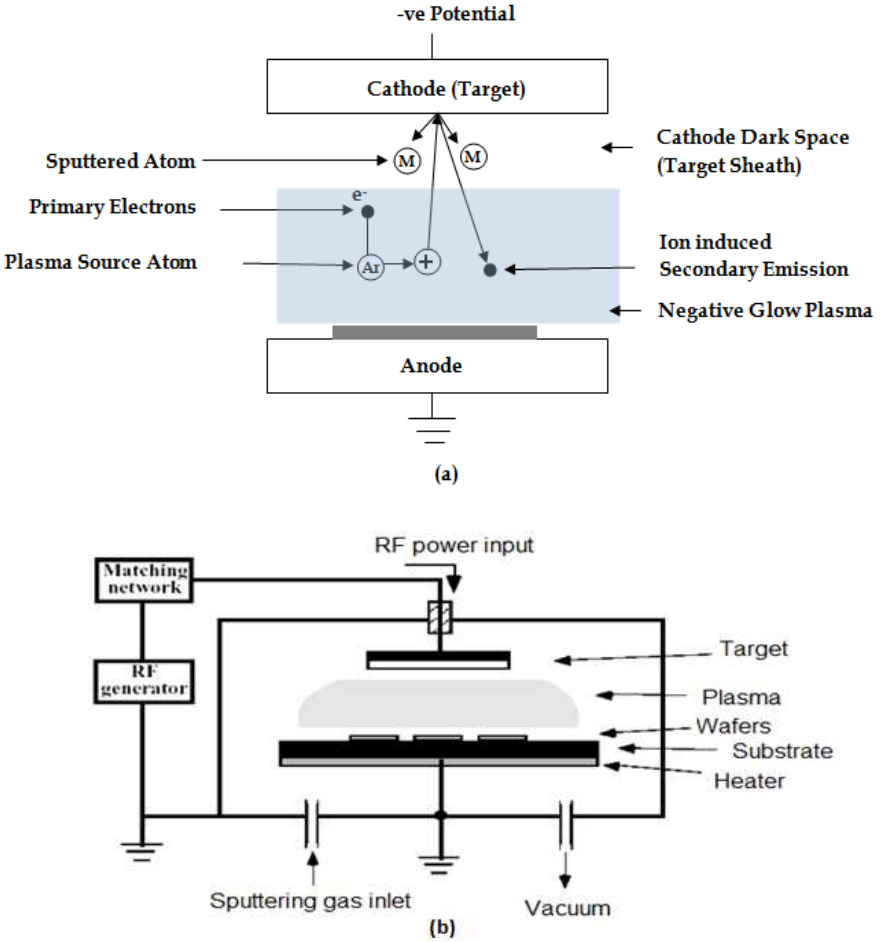

Fig. 1. Schematic Diagrams of (a) DC sputtering and (b) RF sputtering (Ohring, 2002)

In DC sputtering, the target must be electrically conductive otherwise the target surface will charge up with the collection of Ar^+ ions and repel other argon ions, halting the process. RF Sputtering - Radio Frequency (RF) sputtering will allow the sputtering of targets that are electrical insulators (SiO_2, etc). The target attracts Argon ions during one half of the cycle and electrons during the other half cycle. The electrons are more mobile and build up a negative charge called self bias that aids in attracting the Argon ions which does the sputtering. In magnetron sputtering, the plasma density is confined to the target area to increase sputtering yield by using an array of permanent magnets placed behind the sputtering source. The magnets are placed in such a way that one pole is positioned at the central axis of the target, and the second pole is placed in a ring around the outer edge of the target (Ohring, 2002). This configuration creates crossed *E* and *B* fields, where electrons drift perpendicular to both *E* and *B*. If the magnets are arranged in such a way that they create closed drift region, electrons are trapped, and relies on collisions to escape. By trapping the electrons, and thus the ions to keep quasi neutrality of plasma, the probability for ionization is increased by orders of magnitudes. This creates dense plasma, which in turn leads to an increased ion bombardment of the target, giving higher sputtering rates and, therefore, higher deposition rates at the substrate.

We employed dc magnetron sputtering to deposit AlSb thin films. Fig. 2 shows the schematic diagram of Meivac Inc sputtering system. Al and Sb targets were placed in gun 1 and 2 while the third gun was covered by shutter. Both Al and Sb used were purchase from Kurt J. Lesker and is 99.99% pure circular target with diameter of 2.0 inches and thickness of 0.250 inches.

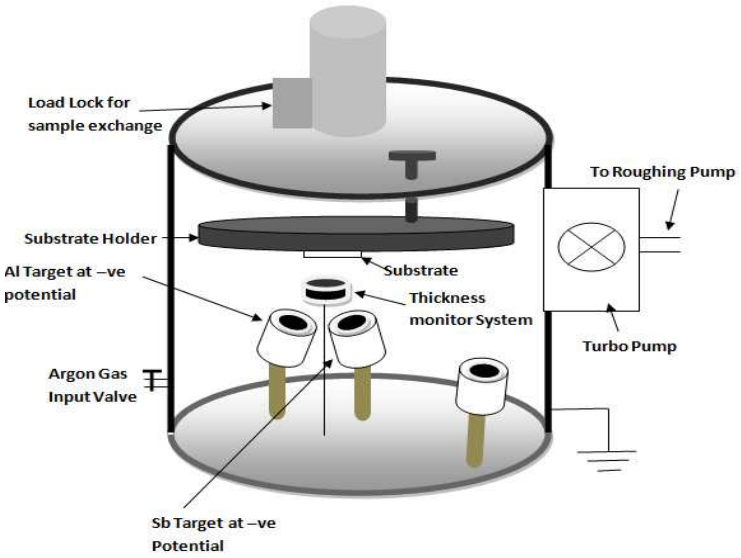

Fig. 2. Schematic diagram of dc magtron sputtering of Al and Sb targets.

Firstly, a separate experiment was conducted to determine the deposition rate of aluminum and antimony and the associated sputtering powers. Al requires more sputtering power than Sb does for depositing the film at same rates. Next Al and Sb was co-sputtered to

produce 1 micron AlSb film in different deposition ratio for Al:Sb. The film was annealed at 200 C in vacuum for 2 hrs and cooled down naturally. Table 1 summarizes the deposition parameters of different AlSb films.

Al: Sb Ratio	Deposition Rate (Å/s)		Sputtering Power (W)		Ar Gas Pressure (mTorr)	Film Thickenss (kÅ)
	Al	Sb	Al	Sb		
1:3	2	6	104	37	20.1	10
2:5	2	5	104	33	20.1	10
3:7	3	7	150	42	20.1	10
1:1	1	1	150	24	20.1	10
7:3	7	3	261	24	20.1	10

Table 1. Deposition Parameters of Different AlSb films.

The film was deposited on glass slides for electrical and optical characterization. The microscopic glass substrate (1 cm x 1 cm) was cleaned using standard substrate cleaning procedure as follows: soaked in a solution of 90% boiling DI and 10% dishwashing liquid for five minutes, followed by soaking in hot DI (nearly boiled) water for five minutes. The substrate was then ultra sonicated, first in Acetone (Fisher Scientific) and then isopropyl alcohol (Fisher Scientific) for 10 minutes each. The substrate was then blown dry with nitrogen.

The morphology of the AlSb film was checked by SEM and was used to validate the grain size and crystalline nature of AlSb particles and shown in Fig. 3.

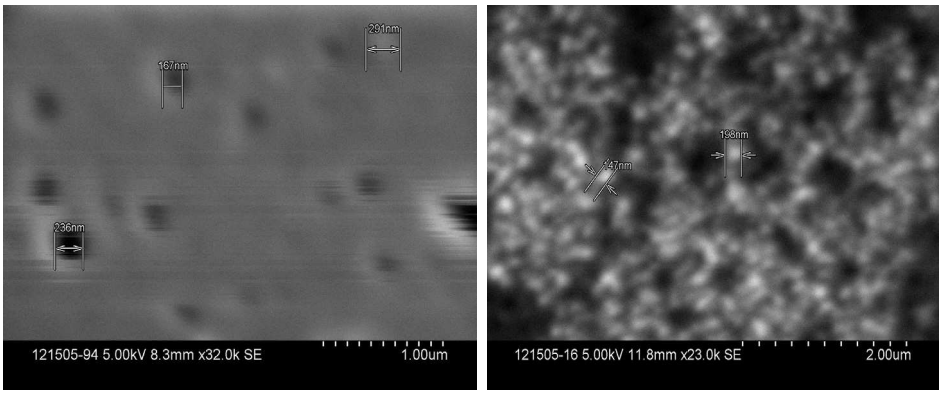

(a) (b)

Fig. 3. SEM images of the AlSb thin film (a) before annealing, and (b) after annealing.

The AlSb grains were found to have been developed after annealing of the film due to proper diffusion and bonding of Al and Sb. Only low magnified image could be produced before annealing the film and holes were seen on the surface. The AlSb microcrystal is formed with an average grain size of 200 nm. Also seen are holes in the film which are primarily the defect area, which could act as the recombination centers. Better quality AlSb film could be produced if proper heating of the substrate is employed during deposition process.

3. Optical characterization of AlSb thin film

The transmittance in the thin film can be expressed as (Baban et al. 2006):

$$T = \frac{I_T}{I_0} = (1-R1)(1-R2)(1-R3)(1-S)e^{-\alpha d} \quad (1)$$

Where, a is the absorption coefficient antd d is the thickness of the semiconductor film. $R1$, $R2$ and $R3$ are the Fresnel power reflection coefficient and the Fresnel reflection coefficient at semiconductor - substrate and substrate – air interface. S measures the scattering coefficient of the surface.

UV Visible Spectrophotometer (Lambda 850) was used to measure the absorption and transmission data. This system covered the ultraviolet-visible range in 200 – 800 nm. The procedures in the Lambda 850 manual were followed. Figure 4 shows the transmittance spectra of the AlSb thin films. The films have an strong absorption in the visible spectral range up to 550 nm for film with Al:Sb ratio 2:5. Similarly for films with Al:Sb in the ratio of 1:3, 1:1 and 3:7 have strong absorption up to 700 nm. The films were transparent beyond these levels.

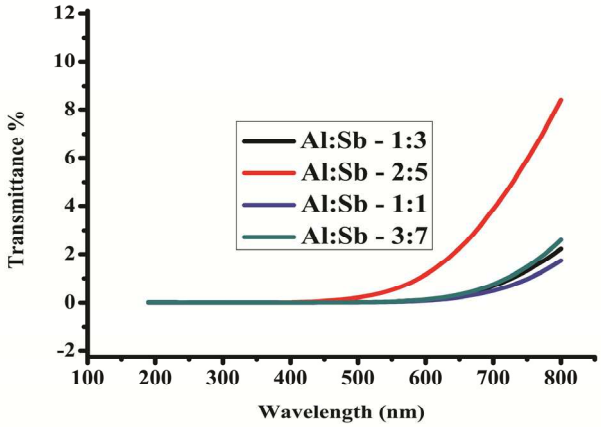

Fig. 4. Transmittance Spectra of AlSb films with different Al:Sb growth ratios.

The film with Al:Sb ratio of 7:3 didn't have a clear transmittance spectra and thus not shown in the figure. This was because the increasing the content of aluminum would make the film metallic thus absorbing most of the light in visible spectrum.

Absorption coefficient of a film can be determined by solving equation 1 for absorption and normalizing the Transmittance in the transparent region as (Baban et al. 2006):

$$\alpha = -\frac{1}{d}\ln\left(T_{normalized}\right) \quad (2)$$

Optical band gap of the film was calculated with the help of transmission spectra and reflectance spectra by famous using Tauc relation (Tauc, 1974)

$$\alpha h\nu = d\left(h\nu - E_g\right)^n \quad (3)$$

Where *Eg* is optical band gap and the constant *n* is 1/2 for direct band gap material and n is 2 for indirect band gap. The value of the optical band gap, *Eg*, can be determined form the intercept of $(\alpha h\nu)^{1/2}$ Vs Photon energy, *hν*, at $(\alpha h\nu)^{1/2} = 0$.

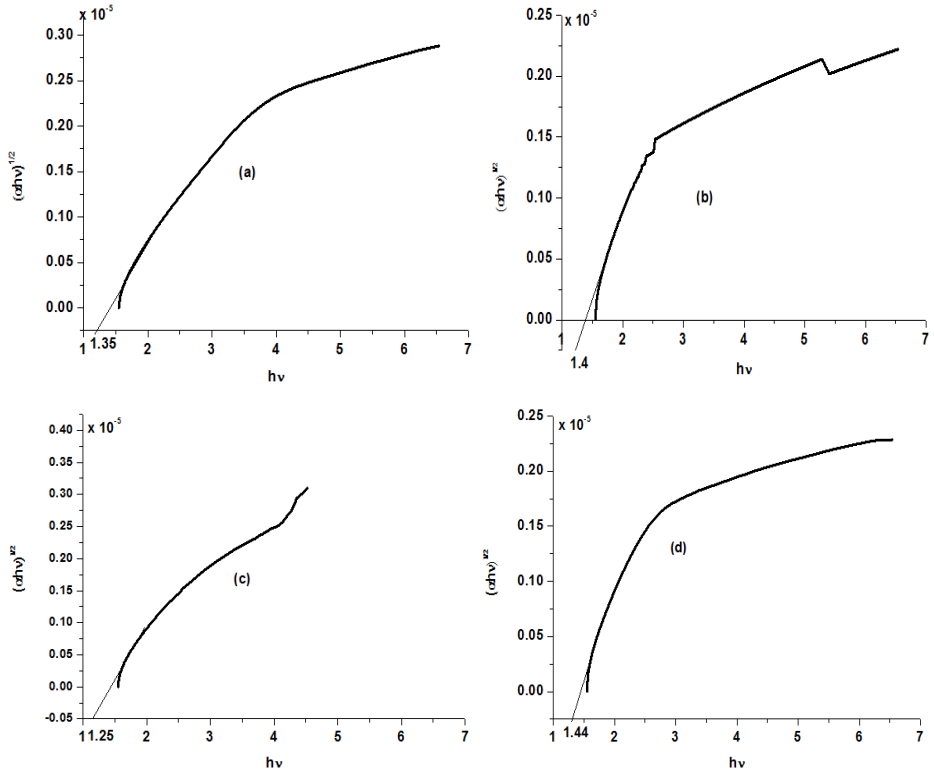

Fig. 5. Bandgap estimation of AlSb semiconductor with Al:Sb growth ratios (a) 1:3, (b) 2:5, (c) 1:1 and (d) 3:7.

The optical absorption coefficient of all the films was calculated from the transmittance spectra and was found in the range of 10^5 cm^{-1} for photon energy range greater than 1.2 eV. Fig. 5 shows the square root of the product of the absorption coefficient and photon energy (*hν*) as a function of the photon energy. The band gap of the film was then estimated by extrapolating the straight line part of the $(\alpha h\nu)^{1/2}$ vs *hν* curve to the intercept of horizontal axis.
This band gap for Al:Sb growth ratio 1:3, 2:5, 1:1 and 3:7 was found out to be 1.35 eV, 1.4 eV, 1.25 eV and 1.44 eV respectively. Since the ideal band gap of AlSb semiconductor is 1.6 eV we have taken the Al:Sb growth ratio to be 3:7 to characterize the film and fabricate the solar cells.

4. Electrical characterization

Material's sheet resistivity, ρ, can be measured using the four point probe method as show in Fig. 6. A high impedance current source is used to supply current (*I*) through the outer two probes and a voltmeter measures the voltage (*V*) across the inner two probes.

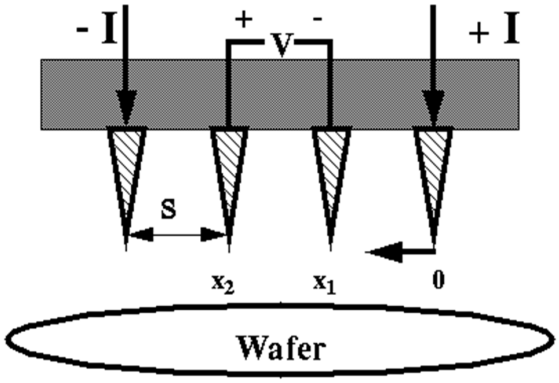

Fig. 6. Schematic diagram of Four point probe configuration.

The sheet resistivity of a thin sheet is given by (Chu et al. 2001):

$$\rho = RCF \frac{V_{measured}}{I_{measured}} \tag{4}$$

Where, RCF is the resistivity correction factor and given by $RCF = \frac{\pi\alpha}{\ln 2}$ The sheet resistance, R_s, could be thus be calculated as $R_s = \rho/d$ and measured in ohms per square. Conductivity (σ) is measured as reciprocal of resistivity and could be related to the activation energy as (Chu et al., 2001):

$$\sigma = \sigma_0 e^{\frac{-\Delta E}{k_b T}} \tag{5}$$

Where, ΔE is the activation energy. This describes the temperature dependence of carrier mobility. The dark conductivity of AlSb film measured as a function of temperature and is shown in Fig. 7.

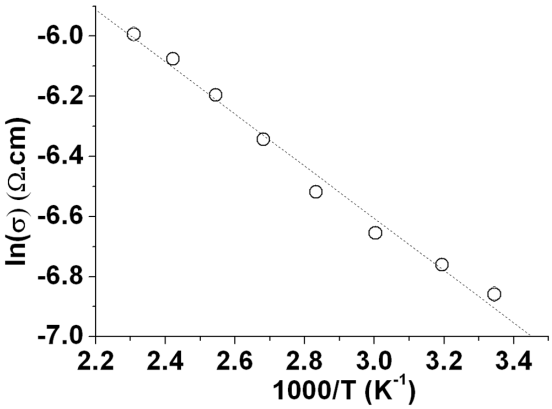

Fig. 7. Temperature dependence of annealed AlSb (3:7) film when heated from 26 - 240 ˚C (dot line for guiding the eyes).

The annealed film shows a linear lnσ vs $1/T$ relationship. The activation energy of the dark conductivity was estimated to be 0.68 eV from the temperature dependence of the conductivity curve for AlSb film. This value is in good agreement with work done by Chen et al. (Chen et al., 2008). This curve also confirms the semiconducting property of the AlSb (3:7) film because the conductivity of the film was seen to be increasing with increasing the excitation.

5. Simulation of solar cell

AMPS 1D beta version (Penn State Univ.) was used to simulate the current voltage characteristics of p-*i*-n junction AlSb solar cells. The physics of solar cell is governed by three equations: Poisson's equation (links free carrier populations, trapped charge populations, and ionized dopant populations to the electrostatic field present in a material system), the continuity equations (keeps track of the conduction band electrons and valence band holes) for free holes and free electrons. AMPS has been used to solve these three coupled non-linear differential equations subject to appropriate boundary conditions. Following simulation parameters was used for the different layers of films.

Contact Interface				
Barrier Height (eV)	0.1 (E_C-E_F)		0.3 (E_F-E_V)	
S_e (cm/s)	1.00×10^8		1.00×10^8	
S_h (cm/s)	1.00×10^8		1.00×10^8	
* S surface recombination velocity of electrons or holes.				
Semiconductor Layers				
	CuSCN	**AlSb**	**ZnO**	**TCO**
Thicknesses, **d** (nm)	100	1000	45	200
Permittivity, $\varepsilon/\varepsilon_0$	10	9.4	10	9
Band gap, E_g (eV)	3.6	1.6	2.4	3.6
Density of electrons on conduction band, N_C (cm^{-3})	1.80×10^{18}	7.80×10^{17}	2.22×10^{18}	2.22×10^{18}
Density of holes on valence band, N_V (cm^{-3})	2.20×10^{19}	1.80×10^{19}	1.80×10^{19}	1.80×10^{19}
Electron mobility, μ_e (cm^2/Vs)	100	80	100	100
Hole mobility, μ_p (cm^2/Vs)	25	420	25	25
Acceptor or donor density, N_A or N_D (cm^{-3})	$N_A = 1\times 10^{18}$	$N_A = 1\times 10^{14}$	$N_D = 1.1\times 10^{18}$	$N_D = 1\times 10^{18}$
Electron affinity, X (eV)			4.5	4.5
* $\varepsilon_0 = 8.85\times10^{-12}$ F/m electric constant; TCO is In_2O_3: SnO_2.				
Gaussian Midgap defect states				
N_{DG}, N_{AG} (cm^{-3})	$A = 1\times 10^{19}$	$D = 9\times 10^{10}$	$A = 1\times 10^{19}$	$D = 1\times 10^{16}$
W_G (eV)	0.1	0.1	0.1	0.1
σ_e (cm^2)	1.00×10^{-13}	1.00×10^{-8}	1.00×10^{-16}	1.00×10^{-11}
σ_p (cm^2)	1.00×10^{-13}	1.00×10^{-11}	1.00×10^{-13}	1.00×10^{-14}

* $N_{DG/AG}$ the donor-like or acceptor-like defect density, W_G the energy width of the Gaussian distribution for the defect states, τ carrier lifetime, and σ capture cross section of electrons (σ_e) or holes (σ_p).

Table 2. Parameters of the simulating the IV behavior or p-*i*-n junction solar cells.

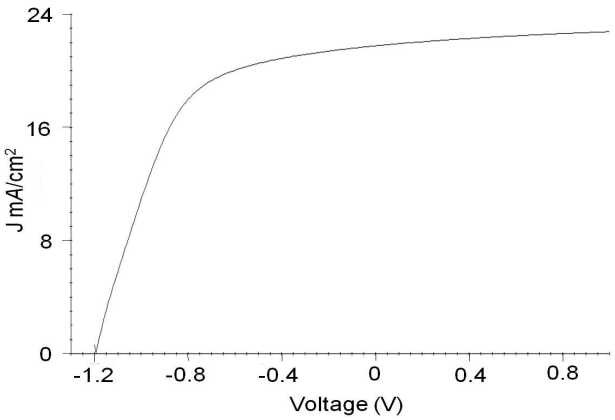

Fig. 8. Current-voltage simulation of AlSb p-i-n junction structure in AMPS 1D software.

Fig. 8 shows the current voltage simulation curve of pin junction solar cell - CuSCN/AlSb/ZnO with AlSb as an intrinsic layer. CuSCN was used as a p layer and ZnO as a n layer. The cell was illuminated under one sun at standard AM 1.5 spectrum.
The simulation result shows that the solar cell has the FF of 55.5% and efficiency of 14.41%. The short circuit current for the cell was observed to be 21.7 mA/cm² and the open circuit voltage was observed to be 1.19 V. AlSb is thus the promising solar cell material for thin film solar cells. The efficiency of the same cell structure could be seen increased up to 19% by doubling the thickness of AlSb layer to 2 micron.

6. Solar cell fabrication

Both p-n and p-*i*-n junction solar cells were designed and fabricated in 1cm x 2 cm substrate with AlSb as a p type and an absorber material respectively. Variety of n type materials including TiO_2 and ZnO were used to check the photovoltaic response of AlSb thin film. Fig. 9 shows the p-n and p-*i*-n based solar cell design with ZnO and TiO_2 are an n-type layer and CuSCN as a p-type layer.

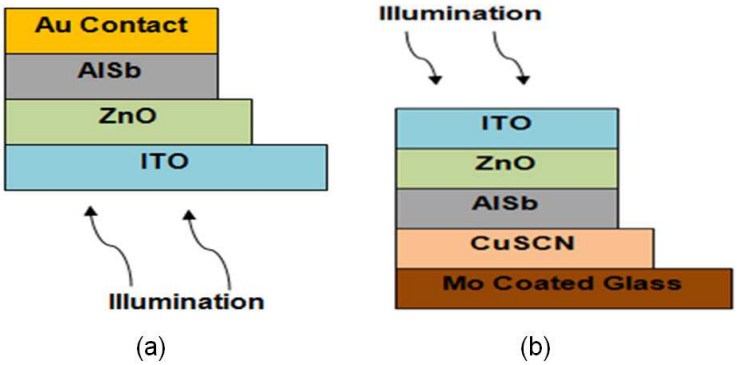

Fig. 9. Solar Cell Design (a) p-n and (b) p-*i*-n structure.

ZnO thin film was prepared by RF sputtering of 99.999% pure ZnO target (Kurt J. Lesker, PA, diameter 2 inches and thickness 0.25 inches). ZnO intrinsic film was deposited by RF power of 100 W at 0.7 Å/s and subsequently annealed in air at 150 ^{0}C. ITO film was also prepared from 99.99% pure ITO target (Kurt J. Lesker, PA, diameter 2 inches and thickness 0.25 inches) on the similar fashion using dc magnetron sputtering. Transparent ITO film was deposited at plasma pressure of 4.5 mTorr. The sputtering power of 20 W yields deposition rate 0.3 Å/s. The film was then annealed at 150 ^{0}C in air for 1 hour. The highly ordered mesoporous TiO_2 was deposited by sol gel technique as described by Tian et al. (Tian et al. 2005). CuSCN thin film was prepared by spin coating the saturated solution of CuSCN in dipropyl sulphide and dried in vacuum oven at 80 ^{0}C (Li et al., 2011). The thickness of all three films ZnO, ITO and TiO_2 film was about 100 nm and the thickness of AlSb layer is ~1 micron. The active layer was annealed.

7. I-V Characterization of solar cell

Current voltage measurement of the solar cells was carried out using Agilent 4155c (Agilent, Santa Clara, CA) semiconductor parameter analyzer equipped with solar cell simulator in SDSU. Fig. 10 shows the experimental set up used for measuring I-V response of the solar cells, where 2 SMUs (source measurement unit) were used. The SMU s could operate as a voltage source (constant sweep voltage) or a current source and it could measure voltage and current at the same time. The SMUs could measure from 10^{-12} A to 1 A and -10 V to 10 V. SMU 1 was set as voltage sweep mode from -1 V to 1 V with steps of 0.01 V, and SMU 2 was set to measure current of the solar cell during IV measurement. IV responses were measured under both dark and illuminated condition. During illumination, the intensity of the simulated light was 100 mW cm^{-2} and calibrated using the NREL calibrated standard cell.

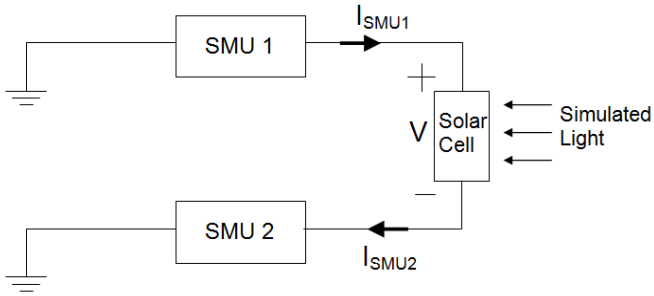

Fig. 10. Experimental set up for measuring IV response of a solar cell.

Table 3 shows the current voltage characteristics of p-n junction solar cells with structures AlSb/TiO_2, AlSb/ZnO. The active cell area was 0.16 cm^2 and fabricated on ITO coated glass surface.

The *V*oc of the best cell with ZnO as an n type layer was found out to be 120 mV and *I*sc to be 76 uA. The *FF* of the cell was calculated to be 0.24 and the efficiency was 0.009%. The cell with TiO_2 as an n layer has even lower V_{OC} and *I*sc. TiO_2 is less suitable n-type layer for making junction with AlSb than ZnO because it is far more conductive than TiO_2. A number of reasons may be attributed for this low efficiency. First, is due to small electric field at the junction between AlSb and the n type material (ZnO or TiO_2). This severely limits the charge

separation at the junction and decreases V_{OC} of the device. A better material needs to be explored to dope AlSb n type to increase the built in field. The field could also be extended using the p-*i*-n structure to design the solar cells.

Cell	V_{OC} (mV)	I_{SC} (mA)	FF	Efficiency %
AlSb/TiO2	80	$12x10^{-3}$	0.23	0.001
AlSb/ZnO	120	$76x10^{-3}$	0.24	0.009

Table 3. Current-voltage characteristics of p-n junction solar cells

Interesting results were obtained with a p-*i*-n junction, CuSCN/AlSb/ZnO. The used cell has an active cell area of this cell was 0.36 cm^2 and fabricated on Mo coated glass surface. Charge was collected from the silver epoxy fingers casted on top of ITO surface and Mo back contact. The cell showed a V_{OC} of ~ 500 mV and a J_{SC} of 1.5 mA/cm^2. With a FF value of 0.5, the efficiency of this cell was calculated to be 0.32%. This observation may be attributed to the more efficient charge separation than that in the p-n junction devices due to a strong build-in field. However, the efficiency of the p-*i*-n junction device is very low in comparison to other available thin film solar cells devices. There are still many unknown factors including the interfaces in the junction. Such a low efficiency could be attributed to the defects along the AlSb interface with both the p- and n-type of layers. Interfaces between AlSb and other layers needed to be optimized for a better performance.

8. Summary

AlSb thin film has been prepared by co-sputtering aluminum and antimony. The deposition rate of Al:Sb was required to be 3:7 to produce the stoichiometric AlSb film with optical band gap of 1.44 eV. After annealing the film at 200 ^{0}C in vacuum for two hours, the film likely formed crystalline structures with a size of ~200 nm and has strong absorption coefficient in the range of 10^5 cm^{-1} in the visible light. p-n and p-*i*-n heterojunction solar cells were designed and fabricated with AlSb as a p-type material and an intrinsic absorber layer. The simulation of the p-i-n junction solar cell with CuSCN/AlSb/ZnO using AMPS at AM1.5 illumination shows efficiency of 14% when setting ~1 μm-thick absorber layer. The p-n junction solar cells were fabricated with different types of n layers shows the photovoltaic responses. The p-*i*-n showed better photovoltaic performance than that of p-n junction cells. All the preliminary results have demonstrated that AlSb is promising photovoltaic material. This work is at the early stage. More experiment is needed for the understanding of the crystallization and properties of the AlSb films and the interface behaviors in the junctions.

9. Acknowledgments

Support for this project was from NSF-EPSCoR Grant No. 0554609, NASA-EPSCoR Grant NNX09AU83A, and the State of South Dakota. Simulation was carried out using AMPS 1D beta version (Penn State University). Dr. Huh appreciates AMES Lab for providing sputtering facility. We appreciate AMPS 1D beta version (Penn State Univ.)

10. References

Aberle, A. G. (2009). Thin Film Solar cells, *Thin Solid Films*, Vol. 517, pp. (4706-4710).

Alsema, E. A. (2000). Energy Pay-back Time and CO_2 Emissions of PV Systems, *Prog. Photovolt. Res. Appl.*, Vol. 8, pp. 17-25.

Andreev, V. M., & Grilikhes, V. A. (1997), *Photovoltaic conversion of concentrated sunlight*, John Wiley and sons, Inc., England.

Armantrout, G. A., Swierkowski, S. P., Sherohman, J. W., &Yee, J. H., 1977, *IEEE Trans. Nucl. Sci.,* NS-24, Vol. 121.

Baban, C., Carman, M., & Rusu, G. I. (2006) Electronic transport and photoconductivity of polycrystalline CdSe thin films, *J. Opto. Elec. and Adv. Materials*, Vol. 8, No. 3, pp. 917-921.

Bagnall, D. M., & Boreland, M. (2008). Photovoltaic Technologies, *Energy Policy*, Vol. 36, No. 12, pp. 4390-4396.

Bartlett, A. A. (1986). Sustained availability: A management program for nonrenewable resources, *Am. J. Phys.*, 54, pp (398-402).

Carabe, J., & Gandia, J. (2004), Thin – film - silicon solar cells, *Optoelectronics Review*, Vol. 12, No. 1, pp. 1-6.

Catalakro, A. (1982). Investigation on High efficiency thin film solar cells, *Proc. of 16th IEEE Photovoltaic Specialist Conf.*, San Diego (CA), pp. 1421-1422.

Chandra, Khare, S., & Upadhaya, H. M. (1988). Photo-electrochemical solar cells using electrodeposited GaAs and AISb semiconductor films, *Bulletin of Material Sciences*, Vol. 10, No. 4, pp. 323-332.

Chen, W., Feng, L., Lei, Z., Zhang, J., Yao, F., Cai, W., Cai, Y.,Li, W.,Wu, L., Li, B., & Zheng, J. (2008). AlSb thin films prepared by DC magnetron sputtering and annealing, *International Journal of Modern Physics B*, *Vol.* 22, No. 14, pp. 2275-2283.

Chittik, R. C., Alexander, J. H., & Sterling, H. E. (1968). The preparation and properties of amorphous Silicon, *Journal of Electrochemical Society*, Vol. 116, No. 1, pp. (77-81).

Chopra, K. L., Paulson, P. D., & Dutta, V. (2004). Thin Film Solar cells: An Overview, *Prog. Photovolt. Res. Appl.*, Vol. 12, pp. (69-92).

Chu, D. P., McGregor, B. M., & Migliorato, P. (2001), Temperature dependence of the ohmic conductivity and activation energy of $Pb_{1+}y(Zr0_{.3}Ti_{0.7})O_3$ thin films, *Appl. Phys. Letter*, Vol. 79, No. 4, pp. 518-520.

Clarson, D. E. (1977). Semiconductor device having a body of amorphous silicon, *US patent* no. 4064521.

Currie, M. J., Mapel, J. K., Heidel, T. D., Goffri, S., & Baldo, M. A. (2008). High-Efficiency Organic Solar Concentrators for Photovoltaics, *Science*, Vol. 321, No. 5886, pp. 226-228.

Dasilva, F. W. O., Raisian, C., Nonaouara, M., & Lassabatere, L. (1991). Auger and electron energy loss spectroscopies study of the oxidation of AlSb(001) thin films grown by molecular beam epitaxy, *Thin Solid Films*, Vol. 200 pp. 33-48.

Dhakal, R., Kafford, J., Logue, B., Roop, M., Galipeau, D., & Yan, X. (2009). Electrodeposited AlSb compound semiconductor for thin film solar cells, *34th IEEE Photovoltaic Specialists Conference (PVSC)*, Philadelphia, pp. 001699 – 001701.

First Solar, n.d. Available from <http://www.firstsolar.com/company_overview.php>

Francombe, M. H., Noreika, A. J., & Zietman, S. A. (1976). Growth and properties of vacuum-deposited films of AlSb, AlAs and AlP, *Thin Solid Films*, Vol. 32, No. 2, pp. 269-272.

Gandhi, T., Raja, K. S., & Mishra, M. (2008). Room temperature Electro-deposition of aluminum antimonide compound semiconductor, *Electrochemica Acta*, Vol. 53, No. 24, pp. 7331-7337.

Green, M. A., Emery, K., Hishikawa, Y., & Warta, W. (2008). Solar Cell Efficiency Tables (Version 32), *Prog.Photovolt:Res.Appl.*Vol. 16, pp. 61–67.

Johnson, J. E. (1965). Aluminum Antimonide Thin Films by co-evaporation of elements, *Journal of Applied Physics*, Vol. 36, pp. 3193-3196.

Kamat, P. V. (2007). Meeting the Clean Energy Demand: Nanostructure Architecture for Solar energy conversion, *J. Phys. Chem. C,* Vol. 111, pp. 2834-2860.

Lechner, P., & Schade, H. (2002). Photovoltaic thin-film technology based on hydrogenated amorphous silicon, *Prog. Photovolt.,* Vol. 10, pp. 85–97.

Leroux, M. (1980). Growth of AlSb on insulating substrates by metal organic chemical vapor depositon, *Journal of crystal growth*, Vol. 48, pp. 367-378.

Li, Y. Yan, M., Jiang, M., Dhakal, R., Thapaliya, P. S., & Yan, X. (2011), Organic inorganic hybrid solar cells made from hyperbranched phthalocyanines, *J of Photonics Energy,* Vol. 1, No. 011115.

Messenger, R. A., & Ventre, J. (2004). *Photovoltaic systems engineering*, CRC Press, pp (2).

Metal Pages, n.d. Available from <http://www.metal-pages.com/metalprices/indium/>

Noufi, R., & Zweibel, K. (2006). High efficiency CdTe and CIGS solar cells, *Photovoltaic Energy Conversion Conference*, pp. 317-320.

Ohring, M. (2002). Material Science of Thin Films, *Academic Press,* pp. 95-273.

Powalla, M., & Bonnet, D. (2007). Thin-Film Solar Cells Based on the Polycrystalline Compound Semiconductors CIS and CdTe, *Advances in OptoElectronics 2007*, article ID 97545, 6 pages.

Rau, U., & Schock, H. W. (1999). Electronic properties of Cu(In,Ga)Se_2 hetero-junction solar cells – recent achievements, current understanding, and future challenges, *Appl. Phys., A Mater. Sci. Process.*, Vol. 69, No. 2, pp. 131–147.

Sean, E., & Ghassan, E. (2005). Organic-Based Photovoltaics: Towards Low Cost Power Generation, *MRS bulletin*, Vol. 30, No. 1, pp. 10-15.

Singh, T., & Bedi, R. D. (1998). Growth and properties of aluminium antimonide films produced by hot wall epitaxy on single-crystal KCl, *Thin Solid Films,* Vol. 312, pp. 111-115.

Staebler, D. L., & Wronski, C. R. (1977). Estimation of the degradation of amorphous silicon solar cells, *Appl. Phys. Lett.,* Vol. 31, pp. 292–294.

Tauc, J. (1974). Amorphous and Liquid Semiconductors, *New-York: Plenum*, pp. (159).

Tawada, Okamoto, Y., H., & Hamakawa, Y. (1981). a-Si:C:H/a-Si:H heterojunction solar cells having more than 7.1% conversion efficiency, *Applied Physics Letters*, Vol. 39, pp. 237-239.

Tawada, Y., Kondo, M., Okamoto, Y., H., & Hamakawa, Y. (1982). Hydrogenated amorphous silicon carbide as a window material for high efficiency a-Si solar cells, *Solar Energy Mater.* Vol. 6, pp. 299-315.

Tian, B., Li, F., Bian, Z., Zhao, D., & Huang, C. (2005). Highly crystallized mesoporous TiO_2 films and their applications in dye sensitized solar cells, *J. Mater. Chem.*, Vol. 15, pp. 2414-2424.

US energy information administration (2010). Available from <http://www.eia.doe.gov/oiaf/ieo/world.html>.

Wesiz, P. B. (2004). *Basic choices and constraints on long-term energy supplies*, Physics Today.

Wu, X. (2001). 16.5% CdS/CdTe polycrystalline thin film solar cell, *Proceedings of 17th European Photovoltaic Solar energy Conference*, Munich, pp. 995-1000.

Zanzucchi, P., Wornski, C. R., & Clarson, D. E. (1977). Optical photoconductivity properties of discharge produced a-Si, *J. Appl. Phys.*, Vol. 48, No. 12, pp. 5227-5236.

Zheng, H., Wu, L. Li, B., Hao, X., He, J., Feng, L. Li, W., Zhang, J., & Cai, Y. (2009). The electrical, optical properties of AlSb polycrystalline thin films deposited by magnetron co-sputtering without annealing, *Chin. Phys. B*, Vol. 19, No. 12, pp. 127204-127207.

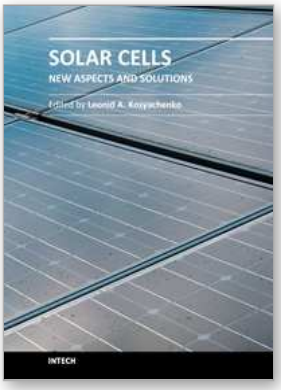

Solar Cells - New Aspects and Solutions

Edited by Prof. Leonid A. Kosyachenko

ISBN 978-953-307-761-1
Hard cover, 512 pages
Publisher InTech
Published online 02, November, 2011
Published in print edition November, 2011

The fourth book of the four-volume edition of 'Solar cells' consists chapters that are general in nature and not related specifically to the so-called photovoltaic generations, novel scientific ideas and technical solutions, which has not properly approved. General issues of the efficiency of solar cell and through hydrogen production in photoelectrochemical solar cell are discussed. Considerable attention is paid to the quantum-size effects in solar cells both in general and on specific examples of super-lattices, quantum dots, etc. New materials, such as cuprous oxide as an active material for solar cells, AlSb for use as an absorber layer in p-i-n junction solar cells, InGaAsN as a promising material for multi-junction tandem solar cells, InP in solar cells with MIS structures are discussed. Several chapters are devoted to the analysis of both status and perspective of organic photovoltaics such as polymer/fullerene solar cells, poly(p-phenylene-vinylene) derivatives, photovoltaic textiles, photovoltaic fibers, etc.

How to reference

In order to correctly reference this scholarly work, feel free to copy and paste the following:

Rabin Dhakal, Yung Huh, David Galipeau and Xingzhong Yan (2011). AlSb Compound Semiconductor as Absorber Layer in Thin Film Solar Cells, Solar Cells - New Aspects and Solutions, Prof. Leonid A. Kosyachenko (Ed.), ISBN: 978-953-307-761-1, InTech, Available from: http://www.intechopen.com/books/solar-cells-new-aspects-and-solutions/alsb-compound-semiconductor-as-absorber-layer-in-thin-film-solar-cells

INTECH
open science | open minds

InTech Europe
University Campus STeP Ri
Slavka Krautzeka 83/A
51000 Rijeka, Croatia
Phone: +385 (51) 770 447
Fax: +385 (51) 686 166
www.intechopen.com

InTech China
Unit 405, Office Block, Hotel Equatorial Shanghai
No.65, Yan An Road (West), Shanghai, 200040, China
中国上海市延安西路65号上海国际贵都大饭店办公楼405单元
Phone: +86-21-62489820
Fax: +86-21-62489821